

Isoscalar E0, E1, and E2 strength in ^{44}Ca , ^{54}Fe , and $^{64,68}\text{Zn}$

J. Button, Y.-W. Lui, D.H. Youngblood, X. Chen,¹ G. Bonasera, and S. Shlomo

¹*Department of Radiation Oncology, Medical College of Wisconsin, Milwaukee, Wisconsin*

The giant resonance region from $10 \text{ MeV} < E_x < 62 \text{ MeV}$ in ^{44}Ca , ^{54}Fe , ^{64}Zn , and ^{68}Zn has been studied with inelastic scattering of 240 MeV α particles at small angles, including 0° . Between 70 and 105% of the expected isoscalar E0 strength has been identified below $E_x = 40 \text{ MeV}$ for each of the nuclei. A majority of the Energy Weighted Sum Rule was identified for E0 and E2 ($\approx 70\%$), and nearly half was identified for E1. Between 70 and 104% of the E1 strength has been identified while 60% of E2 strength in ^{54}Fe and ^{68}Zn and 120% of the strength in ^{64}Zn have been identified. The techniques used for the experiments, data analysis, and DWBA calculations are described in Ref. [1] and references therein. The strength distributions are compared with the predictions from HF-RPA calculations with the KDE0v1 interaction [2--5] and are shown in Figs. 1-4 for the respective nuclei.

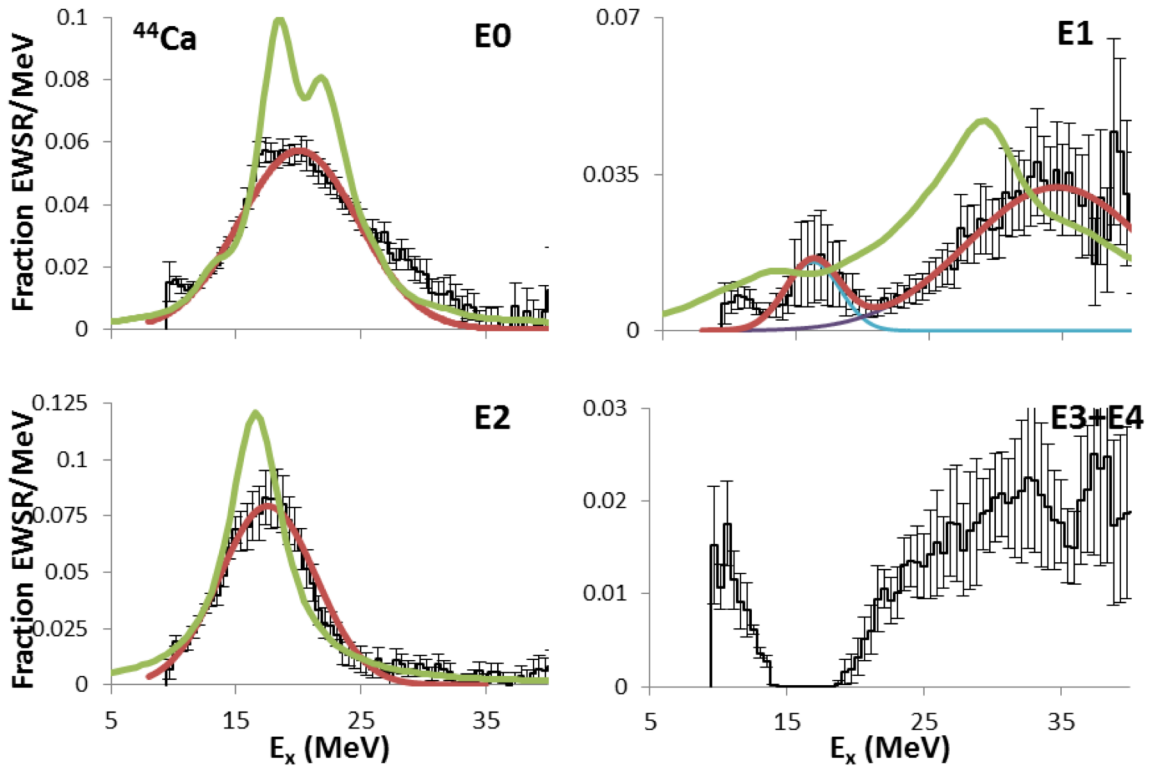


FIG. 1. Strength distributions obtained for ^{44}Ca are shown by the histograms. Error bars represent the uncertainty based on the fitting of the angular distributions and different choices for the continuum. Gaussian fits to the E1 distributions for the individual peaks (blue and purple) and their sum (red) are shown. The green lines are the strength distributions obtained with the HF-RPA calculations using the KDE0v1 interaction, smeared to more closely represent the data.

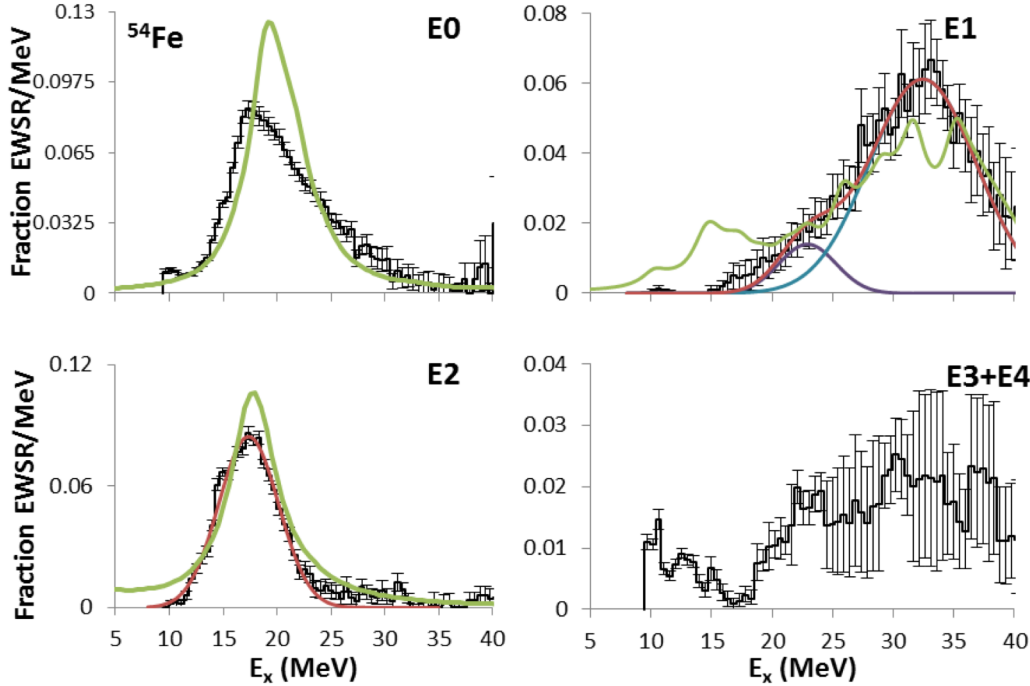


FIG. 2. Strength distributions obtained for ^{54}Fe are shown by the histograms. Error bars represent the uncertainty based on the fitting of the angular distributions and different choices for the continuum. For E1, two Gaussian fits for the low component (purple, smooth line) and high component (blue line) are shown as a sum (red line). A single Gaussian fit is shown for E2. The green lines are the strength distributions obtained with the HF-RPA calculations using the KDE0v1 interaction, smeared to more closely represent the data.

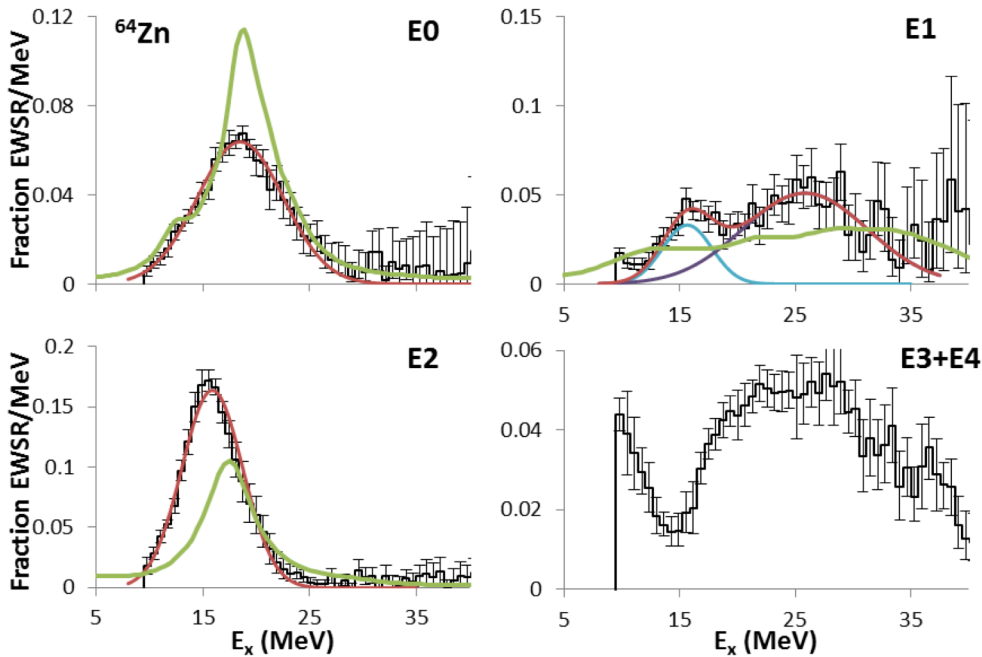


FIG. 3. Strength distributions obtained for ^{64}Zn are shown by the histograms. Error bars represent the uncertainty based on the fitting of the angular distributions and different choices for the continuum. The green lines are the strength distributions obtained with the HF-RPA calculations using the KDE0v1 interaction, smeared to more closely represent the data. The smooth red lines show Gaussian fits.

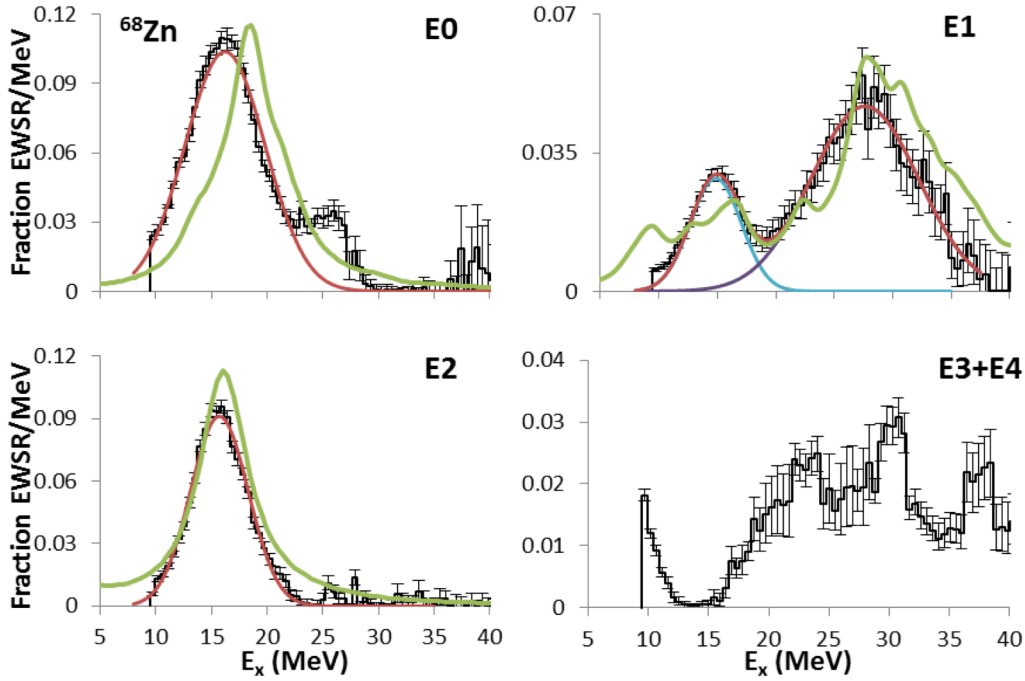


FIG. 4. Strength distributions obtained for ^{68}Zn are shown by the histograms. Error bars represent the uncertainty based on the fitting of the angular distributions and different choices for the continuum. The red, smooth lines show Gaussian fits. The green lines are the strength distributions obtained with the HF-RPA calculations using the KDE0v1 interaction, smeared to more closely represent the data.

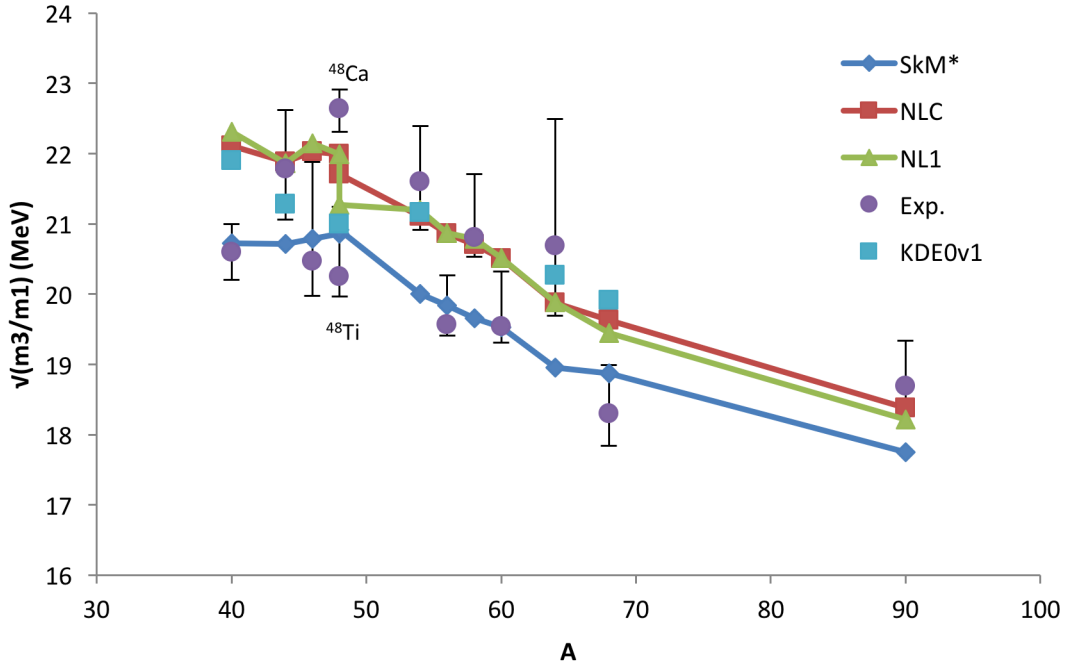


FIG. 5. Experimental GMR energies (represented by solid circles) are compared with values calculated by RMF parameterizations [7] (red squares and green triangles) and Skyrme non-relativistic parameterization [6] (blue diamonds). The error bars on the data include systematic errors. The light blue squares are the values obtained from the KDE0v1 interaction. The experimental energies for $^{40,48}\text{Ca}$ from Ref. [8]; $^{46,48}\text{Ti}$ from Ref. [9], ^{56}Fe , ^{58}Ni , and ^{60}Ni from Ref. [10]; and ^{90}Zr from Ref. [11] are included.

A comparison of the experimental values of the scaling model energy for $E_{\text{GMR}} \left(\sqrt{\frac{m_3}{m_1}} \right)$ with the values calculated from Nayak's [6] calculation based on the SkM*($K_{\text{NM}}=216.6$ MeV), and Chossy and Stocker's [7] calculations based on NLC ($K_{\text{NM}}=224.5$ MeV) and NL1 ($K_{\text{NM}}=211.1$ MeV) non-relativistic and relativistic parameter sets are included in Fig. 5. The ^{54}Fe and ^{64}Zn experimental values agree within the uncertainty with the NLC and NL1 values. The experimental value for ^{68}Zn agrees within uncertainty with the SkM* value and is ~ 1.5 MeV below those calculated with the NLC and NL1 parameter sets. Interestingly, the energies of the GMR in six nuclei (^{40}Ca , $^{46,48}\text{Ti}$, ^{56}Fe , ^{60}Ni , and ^{68}Zn) agree with the SkM* value, while those in six other nuclei ($^{44,48}\text{Ca}$, ^{54}Fe , ^{58}Ni , ^{64}Zn , and ^{90}Zr) agree with the NLC and NL1 values.

- [1] D.H. Youngblood, Y.-W. Lui, J. Button, G. Bonasera, and S. Shlomo, *Phys. Rev. C* **92**, 014318 (2015).
- [2] D.H. Youngblood, Y.-W. Lui, J. Button, M.R. Anders, M.L. Gorelik, M.H. Urin, and S. Shlomo, *Phys. Rev. C* **88**, 021301 (2013).
- [3] M.R. Anders, S. Shlomo, T. Sil, D.H. Youngblood, and Y.-W. Lui, *Phys. Rev. C* **87**, 024303 (2013).
- [4] M. Dutra, O. Lourenço, J.S. Martins, A. Delfino, J.R. Stone, and P. Stevenson, *Phys. Rev. C* **85**, 035201 (2012).
- [5] P. Stevenson, P. Goddard, J. Stone, and M. Dutra, arXiv preprint arXiv:1210.1592 (2012).
- [6] R.C. Nayak, J.M. Pearson, M. Farine, P. Gleissl, and M. Brack, *Nucl. Phys.* **A516**, 62 (1990).
- [7] T.v. Chossy and W. Stocker, *Phys. Rev. C* **56**, 2518 (1997).
- [8] D.H. Youngblood, Y.-W. Lui, and H.L. Clark, *Phys. Rev. C* **63**, 067307 (2001).
- [9] Y. Tokimoto, Y.-W. Lui, H.L. Clark, B. John, X. Chen, and D.H. Youngblood, *Phys. Rev. C* **74**, 044308 (2006).
- [10] Y.-W. Lui, D.H. Youngblood, H.L. Clark, Y. Tokimoto, and B. John, *Phys. Rev. C* **73**, 014314 (2006).
- [11] D.H. Youngblood, H.L. Clark, and Y.-W. Lui, *Phys. Rev. Lett.* **82**, 691 (1999).